Article

ZapA tetramerization is required for midcell localization and ZapB interaction in *Escherichia coli*

Nils Y. Meiresonne[1,#] and Tanneke den Blaauwen[1,*]

[1] Bacterial Cell Biology and Physiology, Swammerdam Institute for Life Sciences, Faculty of Science, University of Amsterdam, Science Park 904, 1098 XH Amsterdam, The Netherlands

[#] Present address: Bacterial Cell Biology, Instituto de Tecnologia Química e Biológica António Xavier, Universidade nova de Lisboa, Oeiras, Portugal

* Correspondence: T.denBlaauwen@uva.nl; Tel.: +31-20-525-3852

Received: date; Accepted: date; Published: date

Abstract:

Bacterial cell division is guided by FtsZ treadmilling precisely at midcell. FtsZ itself is regulated by FtsZ associated proteins (Zaps) that couple it to different cellular processes. ZapA is known to enhance FtsZ bundling but also forms the synchronizing link with chromosome segregation through ZapB and *matS* bound MatP. ZapA exists as dimers and tetramers in the cell. Using the ZapA^{I83E} mutant that only forms dimers, this paper investigates the effects of ZapA multimerization state on its interaction partners and cell division. By employing (fluorescence) microscopy and Förster Resonance Energy Transfer *in vivo* it is shown that; dimeric ZapA is unable to complement a *zapA* deletion strain and localizes diffusely through the cell but still interacts with FtsZ that is not part of the cell division machinery. Dimeric ZapA is unable to recruit ZapB, which localizes in its presence unipolarly in the cell. Interestingly, the localization profiles of the chromosome and unipolar ZapB anticorrelate. The work presented here confirms previously reported *in vitro* effects of ZapA multimerization *in vivo* and further places it in a broader context by revealing the strong implications for ZapB localization and *ter* linkage.

Keywords: Cell division; *ter* linkage, MinC, Z associated protein A (ZapA); Z associated protein B (ZapB); Filamenting temperature sensitive Z (FtsZ);

1. Introduction

ZapA is broadly conserved among Gram-negative and -positive bacteria [1,2]. *E. coli* ZapA promotes FtsZ polymerization through enhancing cooperativity of FtsZ polymer association [3]. However, the turnover of FtsZ is highly dynamic and its filaments would thus not benefit from being rigid when constriction occurs [4]. Many of the ZapA enhanced FtsZ polymerization studies were performed *in vitro* at non-physiological conditions that themselves allow FtsZ to filament and bundle [2]. Experiments performed under physiological conditions revealed a more dynamic stabilizing effect of ZapA on FtsZ bundle formation [3].

An outstanding question is whether the proposed stabilizing effects of ZapA influence FtsZ treadmilling dynamics. Very recently, *in vitro* work showed that transient interactions of ZapA with FtsZ increases the spatial order and stabilizes the architecture of the FtsZ filament network without affecting its treadmilling velocity [5]. These effects were only observed for tetrameric ZapA that was able to interact with FtsZ [5]. ZapA can exist as a mixture of dimers and tetramers *in vitro* but *in vivo* it is likely to be mostly tetrameric due to molecular crowding conditions [3,6,7]. In fact, the available ZapA structures and *in vitro* cross-linking showed a tetrameric structure and tetramerization has already been suggested to be required for FtsZ bundling [6,7,8,9]. These *in vitro* results are interesting but also prompt an *in vivo* explanation of ZapA tetramerization functionality. ZapA acts on FtsZ as a component of the chromosome terminus of replication (*ter*) linkage that synchronizes cell division with chromosome segregation [10]. Indeed, ZapA interacts with ZapB, which interacts with MatP, which binds 23 *matS* sequences distributed on the *ter* domain and condenses this region of the chromosome [11–13]. Therefore, ZapA multimerization dynamics should be investigated in the context of both cell division and chromosome segregation.

Here we describe the molecular behavior of ZapA and its interacting proteins *in vivo*. Dimeric ZapA was unable to complement the ZapA deletion phenotype. Although it did not localize to the division site, it was able to interact with FtsZ elsewhere in the cell, titrating some of it away from midcell. ZapB midcell localization was lost in cells with dimeric ZapA but did not show the same diffuse localization pattern as the ZapA dimers. Instead it resided predominantly at one cell pole suggesting ZapA tetramerization is important for ZapB interaction. Finally, we observed that chromosomal localization is affected in cells without ZapA or with dimeric ZapA as it anticorrelates with the polar ZapB.

2. Results

2.1. Dimeric ZapA^{I83E} does not complement the ΔzapA phenotype

The work of Pacheco-Gómez *et al* [6] shows that ZapA tetramerization is required for FtsZ bundling *in vitro* using ZapA mutant I83E that only forms dimers. This mutant fully folds and forms ZapA dimers that were shown to still bind FtsZ by co-sedimentation [6]. To assess whether ZapA^{I83E} would complement the elongated Δ*zapA* phenotype and restore wild-type morphology *in vivo*, a complementation experiment was performed. Expression of WT ZapA, ZapA^{I83E} or a negative empty vector (EV) control was induced from plasmid with 50 μM IPTG in TB28 Δ*zapA* cells growing in rich medium for ~8 mass doubling as described before [7]. The cells were then fixed, imaged, and average cell lengths were analyzed. This showed that ZapA^{I83E} was unable to complement Δ*zapA* with 6 % of the cells being longer than 10 μm compared to wild type ZapA with 1 % cells longer than 10 μm. ZapA^{I83E} results resembled more the EV control, which had 8 % of the cells longer than 10 μm and ZapA results resembled more the TB28 parental strain with 0.5 % cells longer than 10 μm (**Figure 1**).

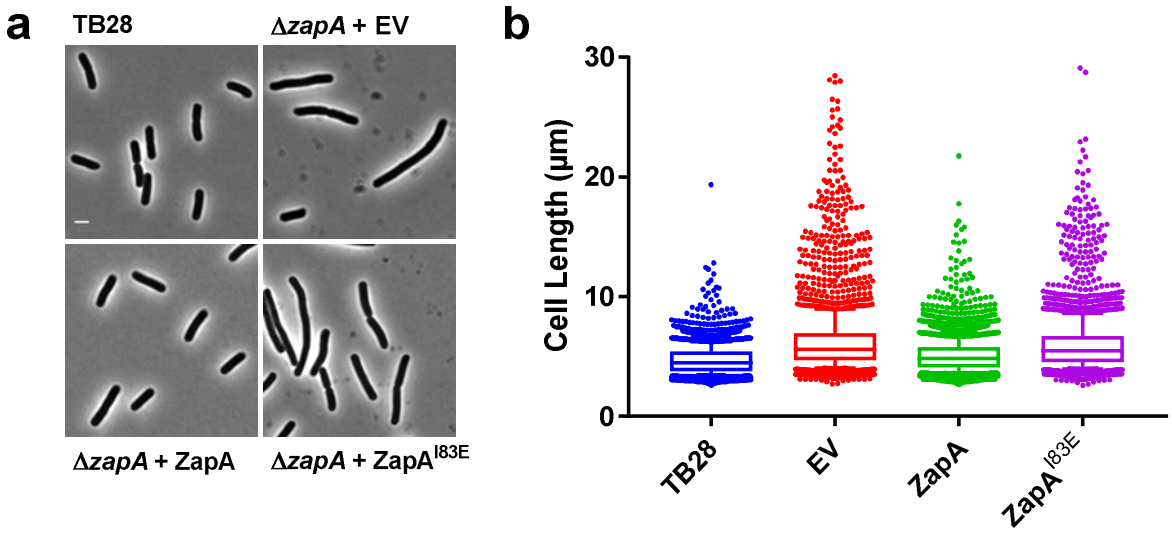

Figure 1 – ZapA^{I83E} does not complement the elongated Δ*zapA* phenotype. (**a**) Phenotypes of the cells. The scale bar represents 2 μm. (**b**) Cell length distributions of each group. The number of cells and their average length measured were for the wild type parental strain TB28; 3670 and 4.5 μm, EV; 2686 and 6.4 μm, from

plasmid expressed ZapA^{WT}; 4476 and 5.1 µm and ZapA^{I83E} ; 2491 and 6.1 µm, respectively. The whiskers represent the 10th and 90th percentile.

2.2. *Dimeric ZapA^{I83E} does not localize at midcell*

ZapA^{I83E} was unable to complement a *zapA* deletion strain based on average cell length. *In vitro* work suggested that dimeric ZapA^{I83E} is still be able to bind FtsZ [6]. Therefore, it was hypothesized that ZapA^{I83E} would localize with FtsZ at midcell and that this may obstruct proper divisome functionality. The Δ*zapA* cells from the complementation experiment were immunolabeled with antibodies against FtsZ, ZapA, or ZapB and a fluorescent secondary antibody to probe their localization patterns. This revealed that ZapA^{I83E} localized throughout the cell, apparently unable to bind FtsZ at midcell (**Figures 2, S1**). FtsZ localized regularly at midcell for all cultures but also more diffusely for the Δ*zapA* and the ZapA^{I83E} cells. Since ZapB midcell localization is dependent on ZapA [7,14] and both proteins are reported to oscillate together between the cell poles [15], it was expected to localize diffusely through the cells expressing dimeric ZapA^{I83E}. Instead ZapB localized polarly in these cells mimicking the pattern of cells without ZapA [7,15]. This sets ZapA^{I83E} apart from the other non-complementing ZapA mutants that did localize to midcell and recruited ZapB [7]. The ZapB localization pattern is a good indication whether ZapA complements at midcell (**Figure S2**).

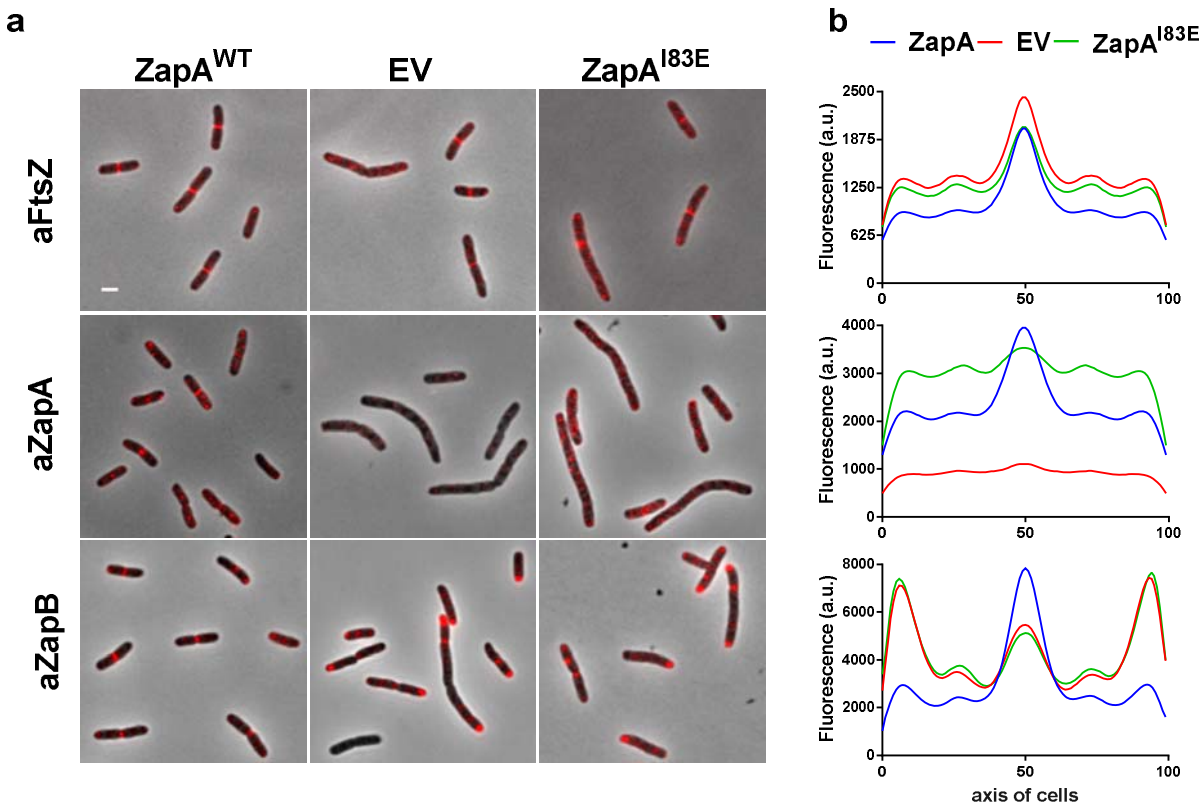

Figure 2 – ZapA^{I83E} does not localize at midcell and does not complement based on ZapB localization. (**a**) TB28 Δ*zapA* cells expressing ZapA^{WT}, an EV control or ZapA^{I83E} were immunolabeled with antiFtsZ, antiZapA and antiZapB and a fluorescent secondary antibody (red). The fluorescence signals from the cells were imaged and analyzed using ObjectJ [16]. The fluorescence intensities are shown at identical brightness and contrast values and the scale bar represents 2 μm. (**b**) The average fluorescence profiles along the cell axis reveal FtsZ midcell localization for all groups. ZapA^{I83E} is expressed and detectable and follows the localization distribution pattern of the EV negative control. Consequently, strong ZapB midcell localization was not observed for ZapA^{I83E} and EV. Maps of the fluorescence profiles are shown in **figure S1**.

2.3. Dimeric ZapA^{I83E} interacts with FtsZ in vivo

The *in vivo* ZapA^{I83E} results did not seem to confirm *in vitro* evidence that the dimer still binds FtsZ. However, its diffuse localization pattern does not exclude the possibility that it is still interacting with FtsZ. ZapA^{I83E} may interact with FtsZ that is therefore not capable to polymerize as a part of the Z-ring. Indeed, the lack of FtsZ bundling was one of the conclusions of the *in vitro* work using ZapA^{I83E} [6]. This should not necessarily have major effects on division given the large amount of FtsZ in the cell of which only 1/3 is

involved in formation of the Z-ring. The critical concentration of FtsZ for polymerization *in vitro* is ~ 1 µM, whereas *in vivo* 5 µM is present. The amount of ZapA^{I83E} produced from plasmid is approximately that of the endogenous concentration of 0.4 µM as tetramer [7]. Not only is there 3 times as much FtsZ as ZapA in the cell, FtsZ overexpression if often observed as an attempt to compensate for division defects [17]. To assess the ZapA^{I83E}-FtsZ interaction regardless of its localization pattern *in vivo*, a FRET experiment was attempted.

The interaction between mKO-FtsZ and mCh-ZapA has been demonstrated *in vivo* by FRET with 4.5 % energy transfer [18]. We aimed to compare the FtsZ-ZapA^{WT} interaction to the putative FtsZ-ZapA^{I83E} interaction. The FP-fusions to ZapA^{WT} and ZapA^{I83E} were confirmed to localize and complement exactly as described for the non-fused proteins under the conditions of a FRET experiment. In addition, the presence of endogenous ZapA did not change the localization pattern of ZapA^{I83E} suggesting that the mutant also cannot tetramerize in combination with ZapA^{WT} (**Supplementary text 5.1, Figure S3**). For the FRET experiment the Δ*zapA* strain was used to increase the chances of plasmid expressed mKO-FtsZ and mCh-ZapA to interact. The FRET experiment was performed as described [18,19]. The direct fusion between mKO and mCh forming a tandem as positive control gave 31 % energy transfer (E*f*A). The negative controls consisted of either mCh-ZapA, mCh-ZapA^{I83E} or mCh-PBP1b paired with the non-interacting IM protein mKO-PBP1a and gave low E*f*A values of less than 1.7 %. Together, these controls suggest a good detection range for the performed FRET experiments (**Figure 3**). Wild type mCh-ZapA interacted with mKO-FtsZ showing the expected energy transfer efficiency of 4 %. Interestingly, mCh-ZapA^{I83E} gave very similar E*f*A values and fluorescence spectra underscoring equal expression. The FRET experiments confirm the binding of dimeric ZapA^{I83E} to FtsZ previously shown *in vitro* by Pacheco-Gomes *et al* [6]. The FRET experiment was repeated in the WT strain resulting in similar E*f*A values of 4.5 and 5.5 % for ZapA and ZapA^{I83E}, respectively.

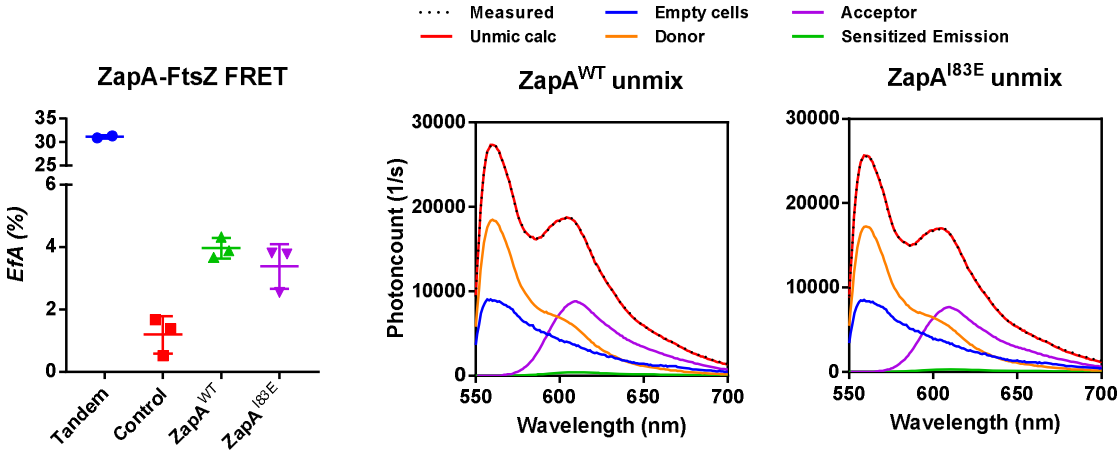

Figure 3 – FtsZ and ZapA^{I83E} *in vivo* interaction FRET assay. On the left the energy transfer efficiency of the indicated FRET pairs. The positive and negative controls suggest a good experiment. On the right typical emission spectra plotted against the photocount for the mCh-ZapA and mKO-FtsZ pairs. The contribution of the direct excitation of mCh (purple) and of mKO (orange) and the background autofluorescence (blue) to the dotted measured spectrum are obtained by the unmixing procedure [18, 19]. The remaining signal (green) is the sensitized emission. mCh-ZapA^{WT} and mCh-ZapA^{I83E} showed similar fluorescence spectra with mKO-FtsZ resulting in very similar E*f*A values.

2.4. ZapB delocalizes unipolarly in cells with dimeric or absent ZapA

ZapB localizes at midcell in wild-type cells but polarly in the absence of ZapA [7,13,15]. In the presence of diffusely localized ZapA^{I83E}, ZapB also localizes polarly instead of following the diffusely distributed pattern. To investigate, TB28 Δ*zapA* containing either ZapA^{WT}, ZapA^{I83E} on plasmids or an EV negative control were grown under minimal medium conditions to prevent large differences in cell length (**Figure S4**). Expression was induced with 50 μM IPTG for at least 2 mass doublings and the cells were fixed and harvested for immunolabeling with antiZapB before imaging. The resulting fluorescence profiles showed the expected ZapB midcell localization in the cells expressing ZapA^{WT} and polar localization for cells expressing ZapA^{I83E} or EV (**Figure 4**). The ObjectJ "poleflipper" macro was used to orient the cell profiles based on the localization of the strongest ZapB signal, reorienting also the underlying channels [16]. This revealed still an average midcell localization of ZapB for the cells expressing ZapA^{WT} but also striking unipolar signals for the

124 cells expressing ZapA^{I83E} or EV (**Figure 4b**). The polar localization of ZapB strongly suggest that ZapA
125 tetramerization is a requirement for its interaction with ZapB.
126

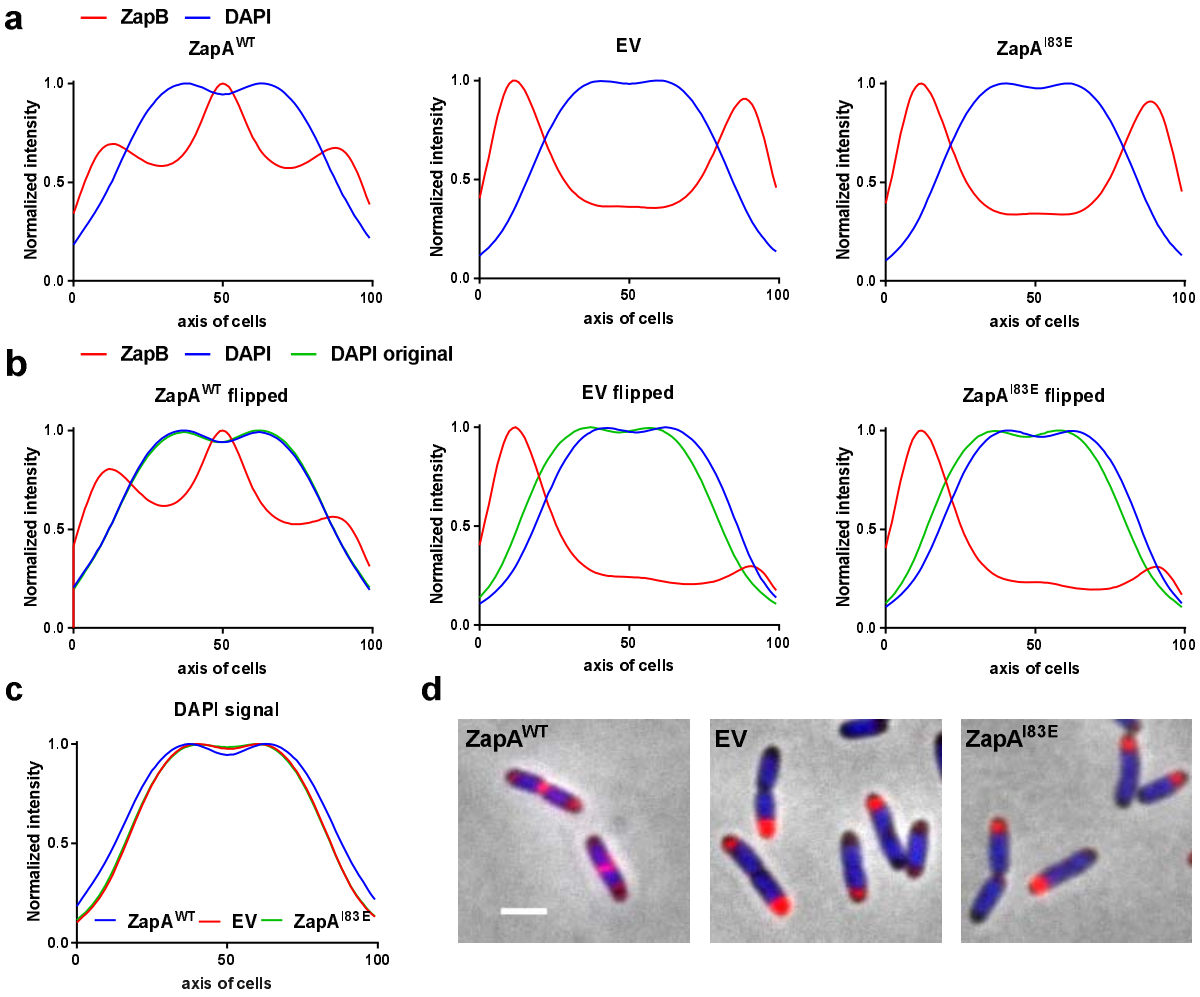

127

128 **Figure 4** - ZapB localizes unipolarly in Δ*zapA* or with plasmid expressed ZapA^{I83E} and is anti-correlating with
129 the chromosomal position. (**a**) Localization profiles of immunolabeled ZapB and DAPI in Δ*zapA* expressing
130 ZapA^{WT}, EV or ZapA^{I83E}. The ZapB profiles show strong signals at midcell in cells with functional ZapA and
131 polar localization in cells without it or with dimeric ZapA. (**b**) When the cells are ordered based on strongest
132 polar signal, predominantly unipolar signals are observed. The DAPI signal in these cells localizes away from
133 ZapB. The blue and green DAPI profiles represent the flipped and non-flipped versions, respectively. (**c**) The
134 DAPI signal in cells without ZapA or with dimeric ZapA seems to be more compacted towards the middle of

the cells and shows less invagination. (**d**) Example of the ZapB immunolabeled (Red) cells with a DAPI stain (Blue). The scale bar represents 2 μm.

2.5 Unipolar ZapB signal anticorrelates with signal for the chromosome.

ZapB interacts with MatP, which connects the chromosomal *ter* region to the divisome [10]. Possibly, its delocalization may influence the chromosome position. To verify this, the Δ*zapA* cells expressing $ZapA^{WT}$, Zap^{AI83E} from plasmid or harboring an EV were visualized with DAPI (**Figure 4a**). When the ZapB poles are flipped, it becomes apparent that the chromosomal signal anti-correlates with the ZapB signal (**Figure 4b**). In the ZapB pole-flipped DAPI profiles for EV and $ZapA^{I83E}$ the chromosome is localized away from ZapB while for cells with $ZapA^{WT}$ the DAPI signal is unaffected. Overlaying the DAPI fluorescence profiles shows that the chromosomes are more localized towards midcell without strong nucleoid invagination for cells without ZapA or with dimeric $ZapA^{I83E}$. Cells expressing $ZapA^{WT}$ show more nucleoid invagination at the site where cell division requires proper nucleoid segregation (**Figure 4c**). The interaction partner of ZapB, MatP, indeed concentrates the *ter* region of the chromosome and a severed *ter* linkage may influence localization and compaction during cell division [11]. This may explain why the DAPI signals show less chromosome invagination in cells with uni-polar ZapB. These observations may provide further insights in *ter* linkage through ZapB function and chromosome segregation. The question remains whether the anti-correlated chromosome is a direct effect of polar ZapB or it is merely occupying the remaining space or do other actors direct the chromosome away from the pole.

2.6 Min oscillation is not affected by polar ZapB, polar ZapB is likely folded and functional

The multimerization state of ZapA is clearly important for *ter* linkage. Because dimeric ZapA is localizing diffusely in the cytoplasm, its oscillation seems to require its interaction with ZapB. However, ZapA seems not to be required for ZapB oscillation as it is still present in the poles and to a much lower extend at mid cell (as it is missing one of its binding partners) (**Figure S5**).

To proof that ZapB is not an inclusion body that is simply obstructing a pole, but is still dynamic, the Δ*zapA* strain and its parental TB28 wild type strain were immunolabelled with antiMinC. Min proteins oscillate from pole to pole where they inhibit Z-ring formation and by a concentration dependent manner allow the proto-ring to form at midcell. Previously, it was shown that the localization pattern of immunolabelled MinC reflects its oscillatory behavior [16]. The MinC pattern was identical in both strains,

165 indicating that MinC completely ignored the presence of ZapB with respect to its position in the cell (**Figure**
166 **5**). These data suggest that the polar ZapB is properly folded and delocalized solely because its midcell
167 recruiting partner ZapA is missing (or dimeric). Indeed, counter-oscillation of FtsZ, ZapA and ZapB has been
168 proposed to build up the new cell division site influenced by Min [15].

169

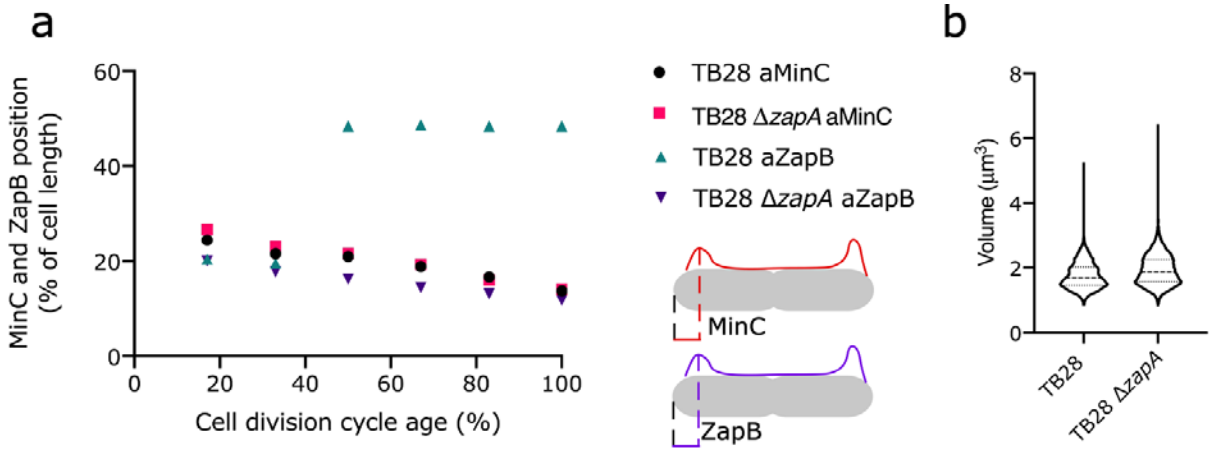

170

171 **Figure 5 –** MinC localization is identical in TB28 and Δ*zapA* despite the polar presence of ZapB in the later
172 strain. (**a**) The distance from the ZapB containing cell pole to the position of MinC in that cell pole was
173 determined in TB28 Δ*zapA* and compared with the position of MinC in wild type cells and plotted against the
174 normalized cell division cycle age (see also cartoon). The position of ZapB in the pole with the strongest ZapB
175 signal in TB28 Δ*zapA* was also plotted and compared to its position in the wild type strain. In the wild type
176 strain, all ZapB molecules end up at mid cell, whereas in the Δ*zapA* strain only a minor amount is present at
177 mid cell (see for complete profiles **figure S5**). (**b**) Volume distribution of TB28 and TB28 Δ*zapA* cells. The
178 number of cells analyzed were for TB28 aMinC, TB28 Δ*zapA* a(anti)MinC, TB28 aZapB, and TB28 Δ*zapA*
179 aZapB 3201, 4154, 3473, and 1726, respectively.

180

181 *2.7 ZapA and MatP effects on ZapB localization*

182 Both ZapB and MatP are required to bring *mats* sites (and thus *ter*) to the division site [20]. If the physical
183 interaction of ZapB and MatP is required for the correct localization of the chromosomes, changes in ZapB
184 dynamics are expected in a Δ*matP* strain. Strain TB28 and Δ*zapA*, Δ*matP* or Δ*zapA* Δ*matP* in the isogenic
185 background were grown in rich medium conditions before they were fixed, harvested and labeled with
186 antiZapB. The fluorescence profiles were flipped and analyzed using ObjectJ (**Figure 6**). As expected, ZapB

187 localized at midcell in the wild-type cells and mostly (uni)polarly in the Δ*zapA* cells. In the absence of MatP,
188 ZapB was still able to be recruited to midcell and partly localized again in the poles and the cells' periphery.
189 The ZapB localization signals are substantially stronger in cells without MatP suggesting either more ZapB
190 production by the cells or more ZapB epitope becomes available to antiZapB. The double deletion strain
191 shows the combined effects of the single *zapA* or *matP* deletions. In these cells, ZapB localizes polarly but also
192 more throughout the cell. This confirms that ZapA guides ZapB to midcell and suggests that MatP keeps
193 ZapB from freely distributing throughout the cell.
194

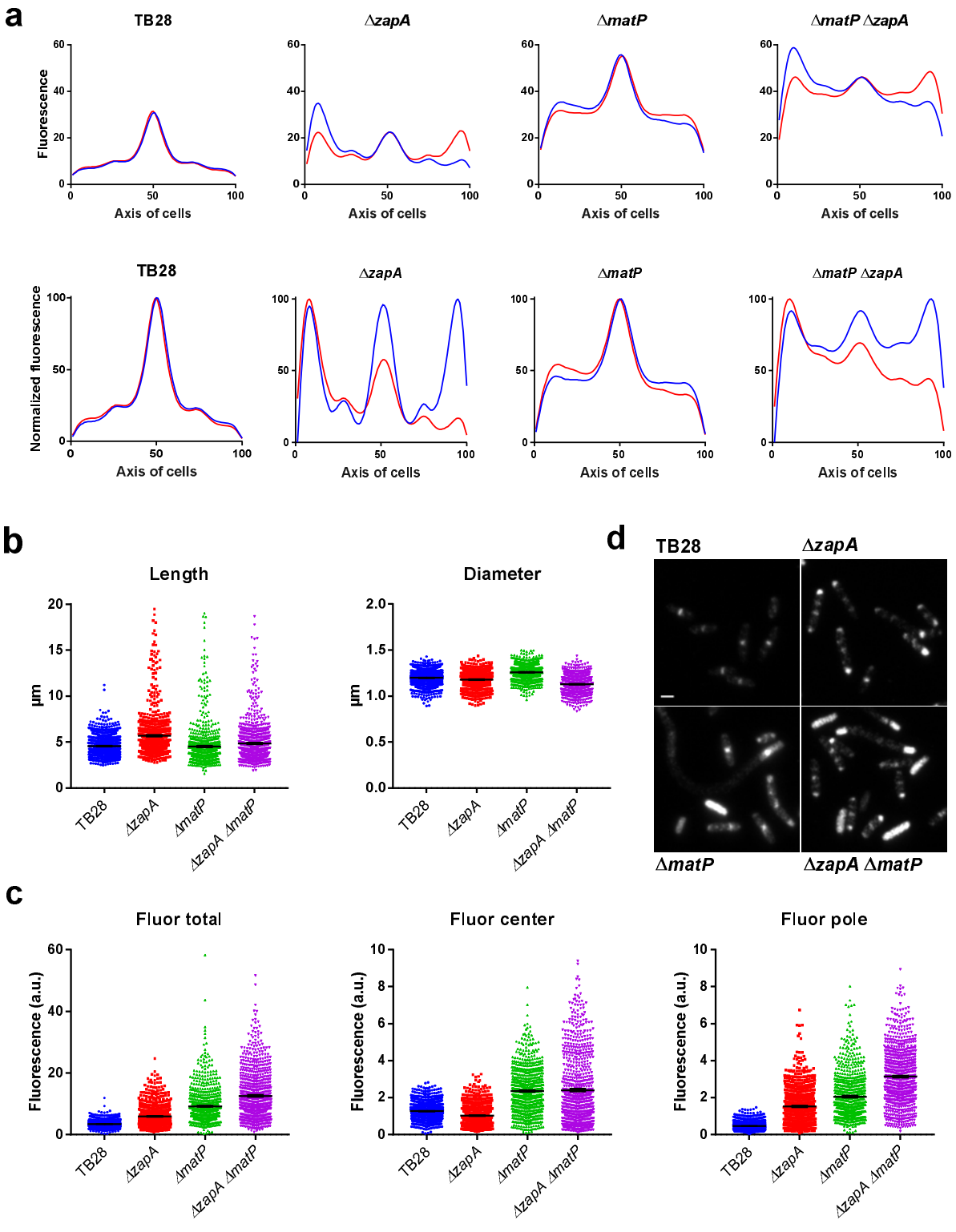

Figure 6 – ZapA is the main factor affecting ZapB localization at midcell. (**a**) Immunolabeled ZapB profiles of TB28, Δ*zapA*, Δ*matP* or Δ*zapA* Δ*matP* grown in rich medium. Absence of MatP has minor effects in ZapB

198 midcell localization but ZapB signals are stronger and localize more throughout the cell. (**b**) Analysis of cell
199 length and diameter show the on average longer cells for Δ*zapA*. (**c**) Subcellular localization of ZapB shows
200 delocalization patterns due to *zapA* and *matP* deletions. The error bars represent the SEM (**d**) Example of the
201 immunolabeled cells. The fluorescence intensities are shown at identical brightness and contrast values and
202 the scale bar represents 2 μm. The number of cells analyzed were for TB28, TB28 Δ*zapA*, TB28 Δ*matP*, and
203 TB28 Δ*zapA* Δ*matP* 1471, 841, 746, and 820, respectively.

204

205 **3. Discussion and conclusion**

206 ZapA is an FtsZ associated protein involved in stabilization of the proto-ring and synchronizing bacterial cell
207 division with chromosome segregation through *ter* linkage. ZapA can exist as tetramers or dimers and *in vitro*
208 evidence suggests its functionality relies on its tetrameric form, even though the dimer can still bind to FtsZ
209 [5,6]. Our work confirms this *in vivo* by investigating tetrameric and dimeric ZapA, as well as FtsZ at the cell
210 division site, and ZapB as the link with chromosome segregation.

211 Although ZapA tetramerization is not a requirement for FtsZ binding, it is for FtsZ binding at midcell.
212 The *in vivo* data suggest that dimeric ZapA only binds cytosolic FtsZ that may therefore be incapable of
213 polymerizing into the proto-ring. Alternatively, the ZapA dimer may be unable to bind FtsZ filaments. The
214 mutant to create dimeric ZapA (I83E), was designed to disrupt the C-terminal multimerization interface to
215 yield parallel ZapA dimers with the globular head group intact but this exact conformation was not verified
216 [6]. Parallel dimeric ZapA is expected to be capable of binding an FtsZ dimer and therefore associate with
217 FtsZ in the proto-ring. Antiparallel ZapA dimerization would weaken the interaction with FtsZ dimers as
218 well as with ZapB explaining the *in vivo* results presented here.

219 Tetrameric ZapA does not interfere with FtsZ protofilament formation and may even be required for its
220 stability [6,12]. A remaining question is whether ZapA tetramerization itself or its interaction with FtsZ at
221 midcell is required for ZapB midcell localization. Other ZapA mutants R13D, E51K and I56K were not
222 complementing cell length but still localized at midcell as did ZapB [7]. This suggested they were interacting
223 with FtsZ and independently still recruited ZapB, apparently affecting the proto-ring in a different manner.
224 The recently published non-complementing ZapA^{R46A} mutation that has been shown to tetramerize but not
225 bind FtsZ may help to answer this question [5,9].

226 ZapB becomes predominantly polar when ZapA is unable to interact with it. When its other interaction
227 partner MatP is absent, more ZapB signal is detectable and still able to localize to midcell but more diffusely
228 and in the cell poles. When both of ZapB's interaction partners are missing, its localization pattern becomes
229 more diffuse and bipolar. This suggests a role for MatP in the unipolar localization of ZapB in Δ*zapA* cells and

continued dynamics if the *ter* linkage is broken. Although speculative, polar ZapB may have a function in WT cells at the beginning of the cell cycle. In this case, ZapB is part of the division ring (*i.e.* not aggregating) and may repulse the DNA after division. The negative charge of ZapB may be of influence on chromosome localization considering it high abundance in the cell [17] with its 17 negative and 8 positive residues this could be significant. However, presently no evidence exists for direct effects of ZapB on the chromosome. A potential way of re-recruitment to the new cell division site is through counter-oscialation with the other early cell division proteins. Only future experiments would lead to a better understanding of ZapB functionality and localization dynamics.

In conclusion, tetramerization of ZapA is required *in vivo* for its binding of FtsZ protofilaments in the Z-ring and for its interaction with ZapB.

4. Materials and Methods

Bacterial strains and growth conditions

Escherichia coli K12 strains used in work are presented in **table 1**. The cells were cultured in rich medium (TY: 10 g Tryptone (Bacto laboratories, Australia), 5 g yeast extract (Duchefa, Amsterdam, The Netherlands) and 5 g NaCl (Merck, Kenilworth, NJ) per liter) supplemented with 0.5% glucose (Merck) or in glucose minimal medium (Gb1: 6.33 g K_2HPO_4 (Merck), 2.95 g KH_2PO_4 (Riedel de Haen, Seelze, Germany), 1.05 g $(NH_4)_2SO_4$ (Sigma, St. Louis, MO), 0.10 g $MgSO_4 \cdot 7H_2O$ (Roth, Karlsruhe, Germany), 0.28 mg $FeSO_4 \cdot 7H_2O$ (Sigma), 7.1 mg $Ca(NO_3)_2 \cdot 4H_2O$ (Sigma), 4 mg thiamine (Sigma), and 4 g glucose per liter, pH 7.0) at 28 °C while shaking at 205 rpm. For growth in Gb1 of TB28 based strains 50 mg lysine, 50 mg arginine, 50 mg glutamine. 20 mg uracil, and 2 mg thymidine (all from Sigma), were added per liter. Expression of protein was induced with isopropyl β-D-1-thiogalactopyranoside (IPTG, Promega, Madison WI) as indicated. Plasmids were maintained in the strains by addition of 100 $\mu g.ml^{-1}$ ampicillin (Sigma) or 25 $\mu g.ml^{-1}$ chloramphenicol (Sigma). Growth was measured by absorbance at 600 or 450 nm with a Biochrom Libra S70 spectrophotometer (Harvard Biosciences, Holliston, MA) for TY or Gb1 cultures, respectively. TB28 Δ*matp* and TB28 Δ*zapA* Δ*matp* were created by P1 transduction of *matp::kan* from the KEIO collection [21] into TB28 and TB28 Δ*zapA*, respectively. The presence of the deletions was confirmed by PCR.

Table 1 – strains used

name	Full name	Reference
DH5α	*F-, supE44, hsdR17, recA1, endA1, gyrA96, thi1, relA1*	[22]
TB28	*rph1 ilvG rfb-50 ΔlacIYZA::FRT*	[23]
TB28 Δ*zapA*	TB28 Δ*zapA*	[14]
sNM02	TB28 Δ*matP*	This work
sNM03	TB28 Δ*zapA* Δ*matP*	This work

Site-Directed Mutagenesis and Plasmid Construction

The plasmids used in this study are shown in **table 2**. Plasmid pGP021 [3] expresses ZapA from a weakened *trc99A* promotor, which is IPTG inducible. The I83E mutation was introduced in the ZapA expressing plasmid pGP016 (6HisZapA) using the Quick change mutagenesis method (Stratagene, la Jolla, CA, USA). The used primers were 5′-GTATGGAACAGCGTGAACGGATGCTGCAGC-3′ and 5′-GCTGCAGCATCCGTTCACGCTGTTCCATAC-3′ and the mutagenesis resulted in plasmid pET302His6ZapA^{I83E}. From this plasmid ZapA^{I83E} was cut using NcoI and HindIII and inserted in pTHV037 to yield plasmid pRP071. Plasmid mCh-ZapA^{I83E} pNM137 was created by exchanging *zapA* in pSAV077 with zapA^{I83E} from pRP071 by restriction digestion cloning using DraIII and HindIII.

Table 2 – Plasmids used in this study

name	Full name/characteristics	Reference
pTHV037	p*trc*99Adown, AmpR, ColE1 ori	[24]
pSAV057	p*trc*99Adown, CamR, P15 ori -	[18]
pGP021	pTHV-ZapA	[3]
pGP016	pET302His6ZapA, p*trc*99A, AmpR, ColE1 ori	[3]
pET302His6ZapA^{I83E}	pET302His6ZapA^{I83E} -	This work
pRP071	pTHV-ZapA^{I83E}	This work
pSAV050	pTHV-mCh-mKO	[18]
pSAV072	pSAV-mKO-FtsZ	[18]
pSAV077	pTHV-mCh-ZapA	[18]
pNM137	pTHV-mCh-ZapA^{I83E}	This work
pBB008	pTHV-mCh-PBP1b	[25]
pBB004	pSAV-mKO-PBP1a	[25]

276

277

278 *Immunolabeling*

279 Immunolabeling of cells was performed described [26] with antibodies against ZapA, FtsZ, or ZapB
280 [16]. The ZapA antiserum was routinely purified by adsorption against TB28 Δ*zapA* cells to filter out
281 potential cross-reactive IgG. The supernatant was subsequently used to label the ZapA mutants.

282

283 *Microscopy and Image analysis*

284 For imaging, the cells were immobilized on 1 % agarose [27] and photographed with a CoolSnap fx
285 (Photometrics) charge-coupled device (CCD) camera mounted on an Olympus BX-60 fluorescence
286 microscope through an UPLANFl 100x/1.3 oil objective (Olympus,Tokyo, Japan). Images were
287 taken using modified acquisition software that used the program ImageJ by Wayne Rasband and
288 analyzed using Object-J's Coli-Inspector [16].

289

290 *FRET assay*

291 The FRET experiments were performed as originally described in [18,19] with the plasmids shown
292 above.

293

294 **Supplementary Materials**: Supplementary materials can be found at XXXX

295

296 **Author Contributions**: Conceptualization, methodology, validation, formal analysis, investigation, data
297 curation, writing—original draft preparation, writing—review and editing, visualization, supervision and
298 project administration were by N.Y.M. and T.d.B.; funding acquisition by T.d.B.

299

300 **Funding**: N.Y.M. was supported by the NWO, ALW open program (822.02.019).

301

302 **Acknowledgments**: We are grateful to René van der Ploeg and Tjalling Siersma for creating the pTHV-ZapA^{I83E}
303 expression plasmid and Elisa Galli for the antiZapB and Miguel Vicente for antiMinC. We thank Jolanda
304 Verheul, Berivan Temiz and Eray Tarhan for technical assistance.

305

306 **Conflicts of Interest**: The authors declare no conflict of interest

307

308

References

1. Gueiros-Filho, F.J.; Losick, R. A widely conserved bacterial cell division protein that promotes assembly of the tubulin-like protein FtsZ. *Genes Dev.* **2002**, *16*, 2544–2556.

2. Small, E.; Marrington, R.; Rodger, A.; Scott, D.J.; Sloan, K.; Roper, D.; Dafforn, T.R.; Addinall, S.G. FtsZ Polymer-bundling by the Escherichia coli ZapA Orthologue, YgfE, Involves a Conformational Change in Bound GTP. *J. Mol. Biol.* **2007**, *369*, 210–221.

3. Mohammadi, T.; Ploeger, G.E.J.; Verheul, J.; Comvalius, A.D.; Martos, A.; Alfonso, C.; Van Marle, J.; Rivas, G.; Den Blaauwen, T. The GTPase activity of Escherichia coli FtsZ determines the magnitude of the FtsZ polymer bundling by ZapA in vitro. *Biochemistry* **2009**, *48*, 11056–11066.

4. Anderson, D.E.; Gueiros-Filho, F.J.; Erickson, H.P. Assembly dynamics of FtsZ rings in Bacillus subtilis and Escherichia coli and effects of FtsZ-regulating proteins. *J. Bacteriol.* **2004**, *186*, 5775–81.

5. Caldas, P.; López-Pelegrín, M.; Pearce, D.J.G.; Budanur, N.B.; Brugués, J.; Loose, M. ZapA stabilizes FtsZ filament bundles without slowing down treadmilling dynamics. *bioRxiv* **2019**, 580944.

6. Pacheco-Gómez, R.; Cheng, X.; Hicks, M.R.; Smith, C.J.I.; Roper, D.I.; Addinall, S.; Rodger, A.; Dafforn, T.R. Tetramerization of ZapA is required for FtsZ bundling. *Biochem. J.* **2013**, *449*, 795–802.

7. Roseboom, W.; Nazir, M.; Meiresonne, N.; Mohammadi, T.; Verheul, J.; Buncherd, H.; Bonvin, A.; Koning, L. de; Koster, C. de; Jong, L. de; et al. Mapping the Contact Sites of the Escherichia coli Division-Initiating Proteins FtsZ and ZapA by BAMG Cross-Linking and Site-Directed Mutagenesis. *Int. J. Mol. Sci. 2018, Vol. 19, Page 2928* **2018**, *19*, 2928.

8. Low, H.H.; Moncrieffe, M.C.; Löwe, J. The Crystal Structure of ZapA and its Modulation of FtsZ Polymerisation. *J. Mol. Biol.* **2004**, *341*, 839–852.

9. Roach, E.J.; Kimber, M.S.; Khursigara, C.M. Crystal Structure and Site-directed Mutational Analysis Reveals Key Residues Involved in Escherichia coli ZapA Function. *J. Biol. Chem.* **2014**, *289*, 23276–23286.

10. Espéli, O.; Borne, R.; Dupaigne, P.; Thiel, A.; Gigant, E.; Mercier, R.; Boccard, F. A MatP-divisome interaction coordinates chromosome segregation with cell division in E. coli. *EMBO J.* **2012**, *31*, 3198–3211.

11. Mercier, R.; Petit, M.A.; Schbath, S.; Robin, S.; El Karoui, M.; Boccard, F.; Espéli, O. The MatP/matS Site-Specific System Organizes the Terminus Region of the E. coli Chromosome into a Macrodomain. *Cell* **2008**, *135*, 475–485.

12. Galli, E.; Gerdes, K. FtsZ-ZapA-ZapB Interactome of Escherichia coli. *J. Bacteriol.* **2012**, *194*, 292–302.

13. Ebersbach, G.; Galli, E.; Møller-Jensen, J.; Löwe, J.; Gerdes, K. Novel coiled-coil cell division factor ZapB

stimulates Z ring assembly and cell division. *Mol. Microbiol.* **2008**, *68*, 720–35.

14. Galli, E.; Gerdes, K. Spatial resolution of two bacterial cell division proteins: ZapA recruits ZapB to the inner face of the Z-ring. *Mol. Microbiol.* **2010**, *76*, 1514–1526.

15. Bisicchia, P.; Arumugam, S.; Schwille, P.; Sherratt, D. MinC, MinD, and MinE drive counter-oscillation of early-cell-division proteins prior to Escherichia coli septum formation. *MBio* **2013**, *4*, e00856-13.

16. Vischer, N.O.E.; Verheul, J.; Postma, M.; van den Berg van Saparoea, B.; Galli, E.; Natale, P.; Gerdes, K.; Luirink, J.; Vollmer, W.; Vicente, M.; et al. Cell age dependent concentration of Escherichia coli divisome proteins analyzed with ImageJ and ObjectJ. *Front. Microbiol.* **2015**, *6*, 586.

17. Li, G.-W.; Burkhardt, D.; Gross, C.; Weissman, J.S. Quantifying Absolute Protein Synthesis Rates Reveals Principles Underlying Allocation of Cellular Resources. *Cell* **2014**, *157*, 624–635.

18. Alexeeva, S.; Gadella, T.W.J.; Verheul, J.; Verhoeven, G.S.; den Blaauwen, T. Direct interactions of early and late assembling division proteins in Escherichia coli cells resolved by FRET. *Mol. Microbiol.* **2010**, *77*, 384–98.

19. Meiresonne, N.; Alexeeva, S.; van der Ploeg, R.; den Blaauwen, T. Detection of Protein Interactions in the Cytoplasm and Periplasm of Escherichia coli by Förster Resonance Energy Transfer. *Bio-Protocol* **2018**, *7*.

20. Lioy, V.S.; Cournac, A.; Marbouty, M.; Duigou, S.; Mozziconacci, J.; Espéli, O.; Boccard, F.; Koszul, R. Multiscale Structuring of the E. coli Chromosome by Nucleoid-Associated and Condensin Proteins. *Cell* **2018**, *172*, 771-783.e18.

21. Baba, T.; Ara, T.; Hasegawa, M.; Takai, Y.; Okumura, Y.; Baba, M.; Datsenko, K.A.; Tomita, M.; Wanner, B.L.; Mori, H. Construction of Escherichia coli K-12 in-frame, single-gene knockout mutants: the Keio collection. *Mol. Syst. Biol.* **2006**, *2*.

22. Bethesda Research Laboratories E. coli DH5 alpha competent cells. *Focus - Bethesda Res. Lab.* **1986**, *8*, 9.

23. Bernhardt, T.G.; de Boer, P.A.J. The Escherichia coli amidase AmiC is a periplasmic septal ring component exported via the twin-arginine transport pathway. *Mol. Microbiol.* **2003**, *48*, 1171–82.

24. Den Blaauwen, T.; Aarsman, M.E.G.; Vischer, N.O.E.; Nanninga, N. Penicillin-binding protein PBP2 of Escherichia coli localizes preferentially in the lateral wall and at mid-cell in comparison with the old cell pole. *Mol. Microbiol.* **2003**, *47*, 539–47.

25. van der Ploeg, R.; Verheul, J.; Vischer, N.O.E.; Alexeeva, S.; Hoogendoorn, E.; Postma, M.; Banzhaf, M.; Vollmer, W.; den Blaauwen, T. Colocalization and interaction between elongasome and divisome during a preparative cell division phase in Escherichia coli. *Mol. Microbiol.* **2013**, *87*, 1074–87.

26. Buddelmeijer, N.; Aarsman, M.; den Blaauwen, T. Immunolabeling of Proteins in situ in Escherichia coli K12 Strains. *BIO-PROTOCOL* **2013**, *3*.

27. Koppelman, C.-M.; Aarsman, M.E.G.; Postmus, J.; Pas, E.; Muijsers, A.O.; Scheffers, D.-J.; Nanninga, N.; den Blaauwen, T. R174 of Escherichia coli FtsZ is involved in membrane interaction and protofilament bundling, and is essential for cell division. *Mol. Microbiol.* **2004**, *51*, 645–57.